



# Experimental and Numerical Study of a Submarine and Propeller Behaviors in Submergence and Surface Conditions

A. Vali<sup>1</sup>, B. Saranjam<sup>2†</sup> and R. Kamali<sup>3</sup>

<sup>1</sup>*Department of Hydrodynamic Research Center, Malek-e Ashtar University of Technology, Shiraz, Iran*

<sup>2</sup>*Air-Naval Complex, Malek-e Ashtar University of Technology, Shiraz, 71855465, Iran*

<sup>3</sup>*School of Mechanical Engineering, Shiraz University, Shiraz, 7193616548, Iran*

†*Corresponding Author Email: [b\\_saranjam@yahoo.com](mailto:b_saranjam@yahoo.com)*

(Received December 16, 2017; accepted April 6, 2018)

## ABSTRACT

In this paper, hull/propeller interaction of a submarine model which has a realistic geometry, in submergence and surface conditions has been studied. For this purpose, the computational fluid dynamics (CFD) method has been used to solve the viscous, incompressible, two phase flow field (in surface condition) around a model of the propeller and submarine hull with and without propeller. The rotation of the propeller has been modeled using the sliding mesh technique. For turbulent flow modeling and free surface simulation, the  $k-\omega$  SST model and the volume of fluid method (VOF) have been used, respectively. Experimental data obtained from test conducted by the authors in M.U.T. towing tank have been used to validate the numerical scheme. Comparing numerical and experimental results shows good agreement. The experimental and numerical results show that operation of the propeller near water surface reduces the thrust coefficient of the propeller comparing to open water condition, so that according to experimental results the maximum relative reduction of the thrust coefficient is 8.95%. In addition, the results indicated the amount of hull resistance coefficient in surface condition is more than submergence condition. According to the thrust reduction and wake factors obtained from the numerical results, it is known that their values in surface condition are less than submergence condition. This research can be used for more realistic investigation of hull/propeller interaction and thus, more accurate powering performance prediction of submarines.

**Key words:** Two phase flows; Hull/propeller interactions; CFD; Sliding mesh; Volume of fluid (VOF) method.

## NOMENCLATURE

$(A_E/A_0)$	blade area ratio	$R_H$	hull resistance
$B$	biass limit	$S$	wetted area
$C_{ht}$	total hull resistance coefficient	$t$	thrust reduction factor
$dh/D$	hub ratio	$T$	propeller thrust
$D$	propeller diameter	$U$	uncertainty
$F$	body force	$U_{inlet}$	inlet velocity
$F_r$	froude number (based on the hull length)	$U_X$	axial velocity
$g$	gravitational acceleration	$\vec{v}$	velocity vector
$J$	advance ratio	$V$	hull advance velocity
$k$	turbulent kinetic energy per unit mass	$\vec{a}$	advance velocity at propeller plane
$K_T$	thrust coefficient	$w$	wake factor
$K_Q$	torque coefficient	$x$	axial distance from propeller plane
$n$	propeller rotation speed (rps)	$Z$	number of blades
$P$	pressure, precision limit	$\alpha$	volume fraction
$(P/D)$	pitch – diameter ratio	$\eta$	propeller efficiency
$Q$	propeller torque	$\vartheta$	kinematic viscosity
$r$	radial coordinate along the propeller blade span	$\vartheta_t$	turbulence eddy viscosity
$R$	radius of propeller	$\rho$	fluid density
$Re$	reynolds number (based on the hull length)	$\omega$	turbulence specific dissipation rate

## 1. INTRODUCTION

Investigating submarine's hull/propeller interaction has great importance for its power estimation. The efficiency of the propulsion system is strongly dependent on propeller performance, thrust force, propeller torque and its efficiency.

Due to strong wake flows behind the hull, especially at high Reynolds numbers, the propeller performance considerably depends on the upward flow conditions (Carlton 2011). Besides, since the flow velocity is not high enough, the presence of the propeller behind the hull can affect the flow condition around the submarine.

In order to analyze flow field around underwater vehicles, both experimental and numerical methods may be used. Experimental methods always have some limitations. They are usually expensive and time consuming. On the other hand numerical methods have gained popularity during the last decades. Compared with experimental methods, numerical methods are considerably less expensive and more efficient if utilized accurately.

Computational fluid dynamics capabilities have been developed during previous years with the development of numerical methods. One of the computational methods which has been used regularly is the potential flow method (Gao and Davies 2002; Kinnas and Hsin 1992; Ohkusu 1996; Ghassemi 2003). However, in this technique the flow is assumed to be inviscid, some of the main characteristics of the flow field such as separation and wake flow cannot be estimated effectively.

Finite volume method is another CFD technique which has been extensively developed. Although, this method is more time-consuming compared with the potential flow method but can lead to more reliable results as shown by Turnock & Wright (2000).

The other computational methods that can be noted are Direct Numerical Simulation (DNS), the Large Eddy Simulation (LES) and Reynolds Average Navier Stokes (RANS). The DNS and the LES are computationally expensive. Hence, marine problems are usually calculated using less expensive methods such as RANS models. One of the most suitable turbulence models in simulating flow field around submarines and propellers is the SST  $k-\omega$  2-equation model which has been used in the current work as well. The SST model performance has been studied in a large number of cases. This model has the advantage of the  $k-\epsilon$  (free flow) and the  $k-\omega$  model (close to wall) (Gohil *et al.* 2016).

The simplest case study of marine propeller is the open water condition. In this case, the performance of propeller at the uniform inflow has been investigated. But in fact, when the propeller is located behind the floating hull, due to flow around the hull, propeller inflow won't be uniform and assuming uniform flow condition around a propeller leads to unrealistic results.

Considering this fact, some studies were done on the prediction of the propeller performance in non-

uniform flow conditions. In some part of these studies the effect of the hull/propeller interaction on the propeller performance was neglected due to the complexity of mesh generation, as well as the large amount of time consuming computations (Watanabe *et al.* 2003; Ji *et al.* 2010; Zhang 2010); Instead, in the absence of the propeller wake behind the hull was considered as the inflow velocity to the propeller. Although this was a useful assumption, it was not accurate because the hull/propeller interaction was ignored in those simulations. The effect of hull/propeller interaction on the propeller performance is considered in another part of these studies.

Hayati *et al.* (2013) investigated the performance of a typical propeller behind an autonomous underwater vehicle in a fully turbulent flow regime at different angles of attack by the application of computational fluid dynamics method.

Nan *et al.* (2005) computed the flow fields around a submarine moving near the free surface. Computed results, including resistances and wave patterns were analyzed.

Simulation of flow on a SUBOFF bare hull model was done by Gross *et al.* (2011). The simulations have been carried out with an in-house developed Navier-Stoke code. In addition, as a reference, RANS calculations were performed using ANSYS CFX. They also investigated the effect of different attack angles of the hull on friction and pressure coefficients.

N. Chase and P. M. Carrica (2013) conducted self-propulsion computations of the DARPA-SUBOFF generic submarine with the E1619 propeller in model scale and analyzed its propulsion performance. They also showed that grid refinement has highly strong effects on the wake calculation.

N. Zhang and S. L. Zhang (2014) studied hull/propeller interaction of a submarine model with a high-skew five blade propeller in submergence and near surface conditions. They evaluated the wave pattern of the submarine model at different depths of submergence. They also computed the thrust, torque and self-propulsion factor of the submarine model in submergence and near surface conditions. In this study the effects of sea waves on the performance of the propulsion system and hull resistance has not been investigated.

Taskar *et al.* (2016) investigated the effect of waves on the propulsion system (propeller & engine), propeller and hull efficiency of a ship. For this purpose an effective method for modeling wake in waves was presented that used to study different aspects of the propulsion system in time varying wake in waves of different wave length, height and direction. This study demonstrates the importance of using a coupled engine propeller system for accurate estimation of ship performance.

G. Budak and S. Beji (2016) investigated the resistance of a DARPA-SUBOFF submarine bare hull and its geometric types using the ANSYS-FLUENT code. For this purpose, three different

bow and three stern forms are generated and nine submarine forms have been created, then the resistance of each submarine form was calculated to determine the best hull.

The resistance and power values of an underwater vehicle (DARPA SUBOFF) have been calculated using both an empirical method and CFD analysis by *Delen et al. (2017)*. In their research, the self-propulsion of the vehicle has been studied using Actuator Disc Theory. In CFD analyses, the flow around DARPA SUBOFF has been solved by Reynolds Averaged Navier-Stokes (RANS) equations using finite volume method (FVM).

Numerical estimation of bank-propeller-hull interaction effect on ship maneuvering has been done by *Kaidi et al. (2017)*. They investigated the influence of ship-bank distance and ship speed on the hydrodynamic forces acting on the ship with and without propeller. Moreover, they computed the impact of the propeller on the hydrodynamic forces acting on the hull.

Existing research study shows that hull/propeller interaction of submarine moving on the water surface has rarely been investigated.

In this paper, the results of experimental tests and numerical simulations of a submarine model which has a realistic geometry with the aim of investigating the hull / propeller interaction in surface and submergence conditions are presented.

The experimental results were used to validate the accuracy of the numerical simulations. The experimental results used in this study were obtained from tests conducted in M.U.T. towing tank of the Republic Islamic of Iran. Dimensions of this tank are 160 m length, 7 m width and 3.5 m height.

In order to carry out numerical simulations, the ANSYS-FLUENT software has been used to solve the viscous incompressible flow field around a model of the propeller and submarine with and without propeller.

## 2. GEOMETRY OF MODELS

The geometrical model of the submarine used in this study is a realistic model of the main components which includes fore planes, tail planes, rudder, sail and ballast tank. This model which has been constructed using CATIA software is shown in Fig. 1. The hull length is equal to 6 m and its height (neglecting the sail) is 0.675 m and also its width at the widest section is 0.71 m. In addition, the sail has a length of 1.125 m and a height of 0.34 m. When the submarine is floating on the water surface, the draught is equal to 0.615 m and the distance of the propeller shaft from water level is equal to 0.252 m (0.9 times the diameter of the submarine propeller).

The Propeller used in this investigation is a skewed five-blade of the Wageningen B-series propeller. The main features of the propeller are documented in Table 1 and the modeled propeller is shown in Fig. 2.

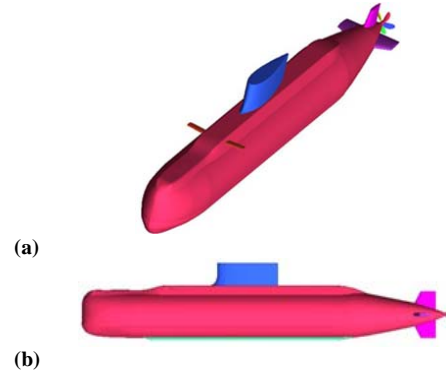


**Fig. 1. Geometrical model of the submarine:**  
a) Isometric view; b) Side view

**Table 1 Main propeller parameters**

Parameters	Values
$Z$	5
Blade area ratio ( $A_E/A_0$ )	0.5
Pitch ratio ( $P/D$ )	0.8
Hub ratio ( $dh/D$ )	0.169
Skew angle ( $^\circ$ )	11.8
Rake angle ( $^\circ$ )	15(Backward)
Diameter ( $D$ )	280mm

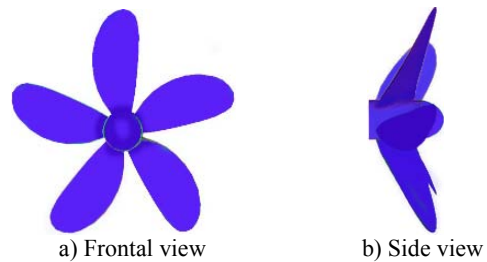


**Fig. 2. Geometrical model of the propeller**

## 3. EXPERIMENTAL TESTS PROCEDURE

In this section, the experimental tests procedures including: propeller in order to determine the performance coefficients, hull resistance under operating conditions on water surface and under water are presented.

As previously mentioned, the experimental tests have been done in the M.U.T. towing tank. This towing tank is illustrated in Fig. 3.



**Fig. 3. M.U.T. towing tank**

It should be noted that making of all models as well as the methods of experimental tests have been carried out on the basis of *ITTC Recommended Procedures and Guidelines (2002a, 2002b, 2002d)*.

### 3.1 Propeller Test

The propeller experiments have been done using the

standard propeller dynamometer fitted to the carriage that tows the propeller dynamometer with a speed which can reach 15 m/s in the towing tank. The calibration of thrust force and torque measured by propeller dynamometer performed statically by calibration weights (ITTC Recommended Procedures and Guidelines (2002c)) and dynamically using a Wageningen propeller due to performance curves being known. Operation specification of the dynamometer that was used to measure the thrust and moment action on propeller and the accuracy of the dynamometer measurement sensors has been presented in Table 2. The experiment was conducted using a 280 mm diameter propeller made with aluminum alloy according to the ITTC Recommended Procedures and Guidelines (2002a).

**Table 2 Maximum operation specifications of propeller dynamometer**

Torque (Nm)	Thrust (N)	Angular velocity (Rpm)	Power (Kw)
55±0.1	1000±2	3000±6	18

In the propeller test in addition to the above mentioned quantities in order to determine the coefficients of propeller performance, advance velocity of towing carriage and water temperature (for calculation of density) have been measured. Data is recorded using an accurate data acquisition system.

The propeller test has been performed in open water condition (at a distance of 0.5 m from the water surface) and near the water surface (at a distance of 0.252 m from the water surface) for advance ratio ( $J = \frac{V}{nD}$ ) from  $J=0.1$  to  $J=0.8$  with 0.1 increments. A view of propeller test has been presented in Fig. 4. The procedure of this test is such that, the propeller with constant rotation is moved through undisturbed water with known forward towing carriage speed. Values of thrust (T) and torque (Q) are gained from the dynamometer, and rate of rotation (n) is recorded by using a tachometer. Measurements are taken during eight series of runs for T & Q at varying J numbers so that n is kept constant and V is varied from speed proportional to  $J = 0.1$  to a high value ( $J=0.8$ ). Then the results are analyzed and performance coefficients are derived.

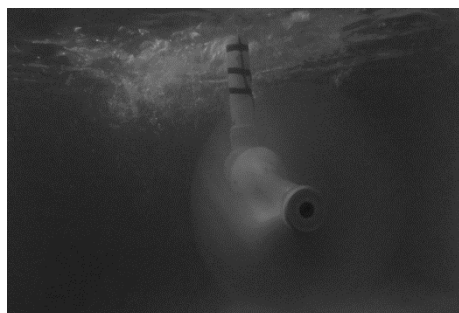


**Fig. 4. Propeller during experimental test near the water surface**

### 3.2 Hull Resistance Test

Determination of the resistance of the hull in surface and submergence conditions has been done according to the procedure provided in this section.

Model used in the hull resistance test has been made, using a structure composed of aluminum and foam as well as fiberglass coat.

#### 3.2.1 Hull Resistance Test in Surface Condition

In order to perform hull resistance test in surface condition a mechanism attached to the towing carriage is used that tows the submarine model with a speed equal to the speed of the towing carriage. This mechanism allows the heave and trim motion of the model and also using a dynamometer connected to it resistance force acting on the model is measured (Fig. 5). In order to avoid the artificial trim effects, the model is attached to the mechanism at the intersection of the propeller thrust line and gravity center line (ITTC Recommended Procedures and Guidelines (2002b)).

This test procedure has been performed such that the model has been accelerated to the desired speed in calm water then the speed has been kept constant for at least 10 seconds. During the test, the measured values of model speed and resistance have been recorded continuously.

The measurement of speed and hull resistance of the model has been carried out using tachometer with ±15mm/s accuracy and 1000N load cell with ±2N accuracy, respectively.

Additionally, water temperature (for calculation of density and viscosity) has been measured and then average values of the measurements for the period of constant speed were calculated.

This process was repeated for other selected speeds and hull resistance test has been obtained for Froude numbers from  $Fr = 0.215$  to  $Fr = 0.435$  with 0.044 increments.

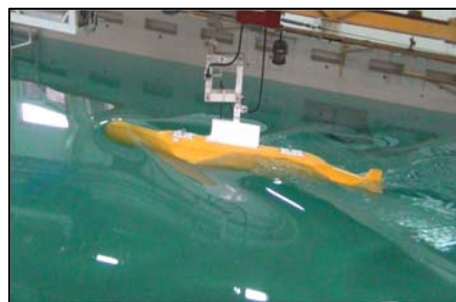


**Fig. 5. Submarine model during the surface test**

#### 3.2.2 Hull Resistance Test in Submergence Condition

Underwater resistance testing of model is done by using a pylon attached to the towing carriage which tows the model. This pylon has a dynamometer to measure the resistance force applied to the model.

Standard depth for fully submerged condition is different in various references (Mooonesun *et al.* 2013). In our experiment in order to reduce the moments of action on the pylon, depth three times the equivalent diameter of the model is used according to the relatively high dimensions of the submarine model, which is less than other values

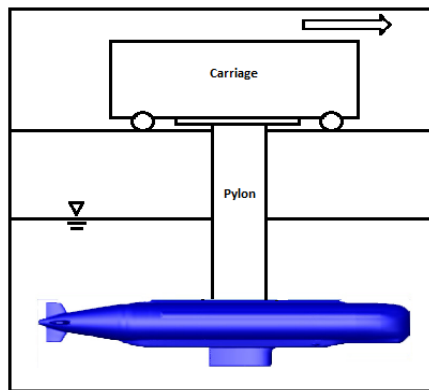
mentioned in the sources.

The values of speed and resistance force are continuously recorded during the test and then the average of these values is calculated. Also, the water temperature is measured in order to determine the physical properties. In the experiment carried out in submergence condition, the same sensors have been used in surface condition.

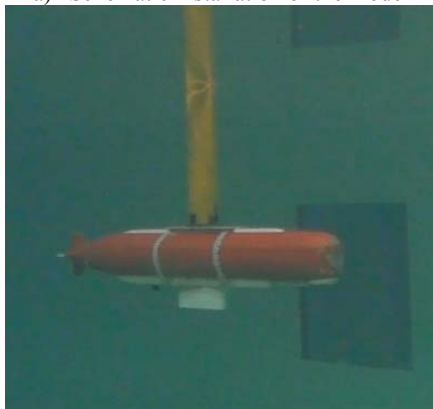
For testing the model in submergence condition, in the first step, the drag force applied to the pylon was obtained in the absence of a submarine model at speeds considered for testing the submarine model. In the next step, the test has been carried out on the model in submergence condition by installing the submarine model on the pylon as shown in Fig. 6. In this case, the model has been installed so that the submarine model sail is toward the bottom of the towing tank in order to reduce the adverse effects of the pylon on the test result as shown in the figure.

The underwater resistance test has been performed in the Reynolds numbers from  $Re = 1 \times 10^7$  to  $Re = 2 \times 10^7$  with  $0.2 \times 10^7$  increments, due to comparison of the results with a similar test in surface condition.

The mentioned test has also been performed in the Reynolds numbers between  $Re = 2 \times 10^7$  to  $Re = 4 \times 10^7$  with  $0.5 \times 10^7$  increments in order to determine the resistance force in all operating range of submarine.



a) Schematic installation of the model



b) Image of model installation in underwater test

**Fig. 6. Installing submarine model in submergence condition**

## 4. NUMERICAL METHOD

### 4.1 Governing Equation

Assuming incompressible and isothermal flow, the continuity and the Navier-Stokes equations in each principal direction are given as:

Continuity equation:

$$\frac{\partial u_i}{\partial x_i} = 0 \quad (1)$$

Momentum equations:

$$\frac{\partial u_i}{\partial t} + u_j \frac{\partial u_i}{\partial x_j} = -\frac{1}{\rho} \frac{\partial p}{\partial x_i} + \frac{\partial}{\partial x_j} \left( (\vartheta + \vartheta_t) \frac{\partial u_i}{\partial x_j} \right) + g_i + \frac{F_i}{\rho} \quad (2)$$

In the above equations,  $u_i$  is the velocity component in each of the principal directions ( $x$ ,  $y$  and  $z$ ),  $\rho$  is the fluid density,  $p$  is the pressure,  $\vartheta$  is the fluid kinematic viscosity and  $\vartheta_t$  is the turbulence eddy viscosity which is found using a turbulence model;  $F_i$  and  $g_i$  represent body forces and gravitational acceleration, respectively.

In the current study, the SST  $k$ - $\omega$  turbulence model was utilized for modeling the flow turbulence. This model was developed first by [Menter \(1994\)](#). The transport equations of this model are as follows:

$$\frac{\partial}{\partial t} (\rho k) + \frac{\partial}{\partial x_i} (\rho k u_i) = \frac{\partial}{\partial x_i} \left( \Gamma_k \frac{\partial k}{\partial x_j} \right) + \widetilde{G}_k - Y_k + S_k \quad (3)$$

$$\frac{\partial}{\partial t} (\rho \omega) + \frac{\partial}{\partial x_i} (\rho \omega u_i) = \frac{\partial}{\partial x_i} \left( \Gamma_\omega \frac{\partial \omega}{\partial x_j} \right) + G_\omega - Y_\omega + D_\omega + S_\omega \quad (4)$$

In these equations,  $\widetilde{G}_k$  represents the generation of turbulence kinetic energy due to mean velocity gradients,  $G_\omega$  represents the generation of  $\omega$ ,  $\Gamma_k$  and  $\Gamma_\omega$  represent the effective diffusivity of  $k$  and  $\omega$  due to turbulence,  $D_\omega$  represents the cross-diffusion term,  $S_k$  and  $S_\omega$  are user-defined source terms.

For modeling the free surface, Volume of Fluid (VOF) method was utilized. The VOF method was originally developed by [Hirt and Nichols \(1981\)](#). The governing equations of the flow field in this method are still the continuity and momentum equations; the fluid properties such as density and kinematic viscosity are defined based on the volume fractions of the phases in each cell though. For two-phase flow the continuity equation includes both phases (water and air). Each phase mass will be conservative. The tracking of the interface between the two phases (free surface) is accomplished by the solution of a continuity equation for the volume fraction. For each phase, this equation has the following form:

$$\frac{\partial \alpha_q}{\partial t} + \vec{v} \cdot \nabla \alpha_q = 0 \quad (5)$$

In this equation  $\alpha_q$  represents the volume fraction of the  $q$ th phase. Obviously, the sum of volume fractions will be equal to one.

Finally, each fluid property in each cell is given as  $\varphi$ :

$$\varphi = \sum \alpha_q \varphi_q \quad (6)$$

### 4.2 Geometry and Domain Discretization

For flow domain discretization, a hybrid mesh around geometric model was generated. Unstructured grid is used near the submarine and propeller, where generating structured elements is quite difficult, while in the far regions the grid is structured. Using the structured grid in far regions reduces the grid size significantly, which has the considerable effect of reducing computational costs. For grid generation ANSYS ICEM software was utilized.

A view of a cylindrical computational domains used in this study is presented in Fig. 7. In this figure  $L$  is the length of submarine and  $D$  is the diameter of propeller.

In this study, sliding mesh technique was utilized to simulate the rotation of the propeller. For this purpose a cylindrical region which encloses the propeller was considered as the moving zone. A 2-dimensional view of moving and stationary mesh zone is shown in Fig. 8.

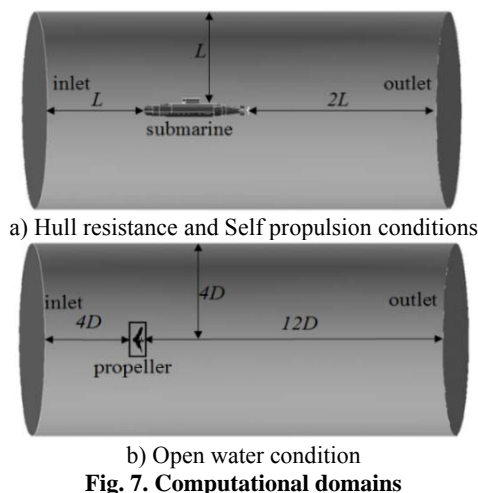


**Fig. 7. Computational domains**

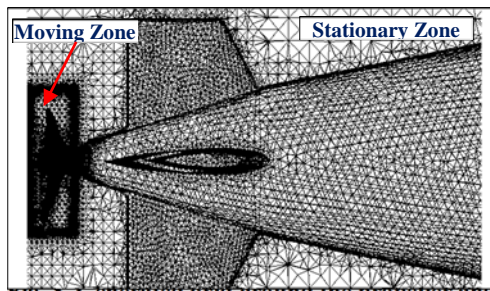


**Fig. 8. Generated grid around the propeller and at the back of the submarine; side view**

For more accurate simulation of turbulent flow on submarine and propeller surfaces, a boundary layer grid consisting of 6 layers of prismatic elements has been generated. Also, propeller blades surfaces were meshed with triangular cells. Smaller triangles with sides of approximately  $0.0025D$  have been used for regions near to the tip, root and blades edges (Rishehri *et al.* 2007). Regions inside the blade meshed with larger triangular cells in which the length of the sides increase gradually with the growth rate of 1.1. Figure 9 shows part of generated grid on surface of the propeller.

For studying the grid independency around the submarine hull in submergence condition, the flow field around the hull has been solved in several networks, numerically analyzed at Reynolds number  $2 \times 10^7$ , and the total hull resistance coefficients obtained are compared with each other.

Results of this study are presented in Table 3, network 3 is used to solve the flow field around the hull for numerical simulation due to the negligible difference between the results of the third and fourth networks as well as lower number of cells in third network knowing that increasing the numbers of cells concludes longer computational time.

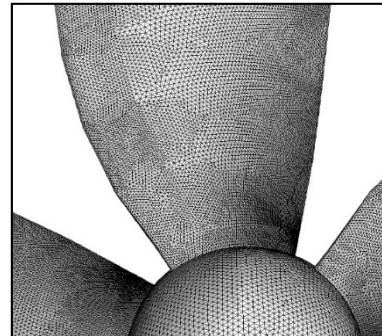


**Fig. 9. A view of the grid generation on the propeller surface**

The number of cells obtained for other simulated models in the present research similar to the previous mentioned grid independency study. Grid study results are shown in Table 4.

**Table 3 Total hull resistance coefficient in terms of the numbers of networks**

Network	Number of cells	Total hull resistance coefficient ( $C_{ht}$ )
1	$1.352 \times 10^6$	$2.87 \times 10^{-3}$
2	$2.098 \times 10^6$	$3.64 \times 10^{-3}$
3	$2.786 \times 10^6$	$3.99 \times 10^{-3}$
4	$3.452 \times 10^6$	$4.01 \times 10^{-3}$

**Table 4 Numbers of cells in the computations**

Condition	Rotational	Stationary	Total
Resistance hull (half domain)	---	$2.786 \times 10^6$	$2.786 \times 10^6$
Open-water	$1.579 \times 10^6$	$1.473 \times 10^6$	$3.052 \times 10^6$
Self-propelled	$1.394 \times 10^6$	$5.457 \times 10^6$	$6.851 \times 10^6$

### 4.3 Flow Solver and Boundary Conditions

As previously mentioned, The CFD package, FLUENT (ANSYS 17) has been used for solving the governing equations for the flow around the submarine and propeller in the submergence and on the water surface conditions.

According to time step independency study, the time step size for solving the unsteady governing equations were set to 0.001 sec and the implicit scheme was utilized for discretizing the time derivative terms. Also, for discretizing the momentum equations and transport equations of the turbulence model, the second order upwind method

was utilized. For coupling between the pressure and velocity field the SIMPLE algorithm was used.

Boundary conditions are set as follows:

At the inlet the velocity was set constant. At the outlet a hydrostatic pressure condition was imposed using a User Defined Function (UDF) implemented in FLUENT. Also, no-slip boundary condition was set on the submarine and propeller surfaces and symmetry condition was imposed at the outer boundary. In surface condition at the inlet, outlet and outer boundary, volume fraction is prescribed (Ref. Fig. 7).

## 5. RESULTS

### 5.1 Submergence Condition

In order to investigate hull/propeller interaction of submarine in submergence condition, performance of propeller in open water condition, hull resistance and the forces of submarine with propeller (self-propulsion Condition) have been studied.

#### 5.1.1 Open Water Performance

Computational performance coefficients ( $K_T$ ,  $K_Q$ ,  $\eta$ ) of the propeller are compared with the experimental results presented by Bernitsas *et al.* (1981) and obtained from this study for various advance ratios in open water condition, and the results are shown in Fig. 10. In order to obtain experimental results in this study, each experimental data obtained with 5 times the test repeat.

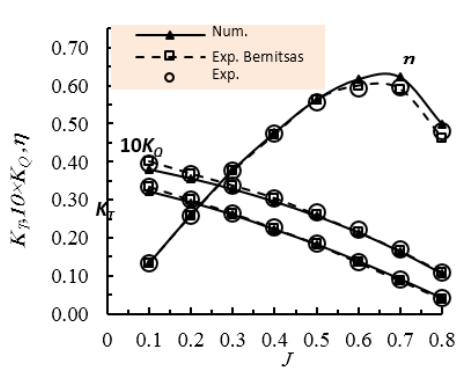


Fig. 10. Computational and experimental performance and efficiency curves of the propeller in open water condition

$K_T$  and  $K_Q$  are the propeller thrust and torque coefficients and  $\eta$  is the propeller hydrodynamic efficiency, which are defined as:

$$K_T = \frac{T}{\rho n^2 D^4} \quad (7)$$

$$K_Q = \frac{Q}{\rho n^2 D^5} \quad (8)$$

$$\eta = \frac{J}{2\pi} \cdot \frac{K_T}{K_Q} \quad (9)$$

Comparing the experimental results obtained from this study with the results of Bernitsas *et al.* (1981) shows a small difference between the results. So that, the maximum difference between the thrust coefficients is 1.4% and the torque coefficients is 2.3%. On the other hand, Comparison of computational results with experimental data obtained from this study, shows that the maximum error of the propeller thrust and torque coefficients are about, 4.4% and 5.3%, respectively. These results show the numerical method good accuracy.

Uncertainty of the experimental results obtained from the propeller tests in open water condition have been presented in Table 5. The uncertainty (U) of the experimental results consists of two components of bias (B) and precision (P), the total bias and precision limits have been obtained by the root sum squared of bias errors and standard deviation of the measured values including propeller geometry, advance velocity, propeller rate of revolution, thrust, torque, and temperature/density, respectively.

#### 5.1.2 Hull Resistance

The hull resistance without propeller in submergence condition has been computed in different Reynolds numbers from  $1 \times 10^7$  to  $4 \times 10^7$ ; and then these results have been compared with results obtained from submarine model's test in the towing tank for verification.

Computational and experimental hull resistance coefficients ( $C_{ht} = \frac{R_H}{0.5 \times \rho \times V^2 \times S}$ ) versus Reynolds numbers (based on the hull length) have been shown in Fig. 11.

The results shown in this figure indicate that relative error of calculated coefficients increases by reducing the Reynolds numbers. So that, in Reynolds  $Re = 1 \times 10^7$ , relative error of computed coefficient reaches to the maximum value (about 4%). The mentioned error has also been seen in N. Zhang and S. L. Zhang (2014) work. They declared accuracy at high speeds, because fully developed turbulence simulation is used in CFD, while there are laminar and transition disturbances in tests with low speed.

Table 5 Uncertainty of the propeller experimental results in open water condition

J	0.1	0.20	0.3	0.40	0.5	0.6	0.7	0.8
$B_{KT}$	1.93E-03	1.85E-03	1.60E-03	1.36E-03	1.08E-03	8.56E-04	5.43E-04	3.14E-04
$P_{KT}$	3.85E-04	3.83E-04	2.90E-04	1.94E-04	1.91E-04	1.61E-04	8.10E-05	4.40E-05
UKT	1.96E-03	1.89E-03	1.62E-03	1.37E-03	1.09E-03	8.71E-04	5.49E-04	3.17E-04
$U_{KT}/K_T(\%)$	0.67	0.70	0.68	0.66	0.64	0.64	0.62	0.79
$B_{KQ}$	2.58E-04	2.55E-04	2.28E-04	1.97E-04	1.63E-04	1.36E-04	9.71E-05	5.77E-05
$P_{KQ}$	1.04E-04	1.04E-04	8.62E-05	5.31E-05	5.40E-05	4.80E-05	2.86E-05	1.60E-05
$U_{KQ}$	2.78E-04	2.75E-04	2.44E-04	2.04E-04	1.71E-04	1.45E-04	1.01E-04	5.98E-05
$U_{KQ}/K_Q(\%)$	0.75	0.79	0.76	0.73	0.71	0.72	0.67	0.75

As mentioned above, the maximum relative error of computed coefficient was considered small, and the CFD result is valid for further analysis.

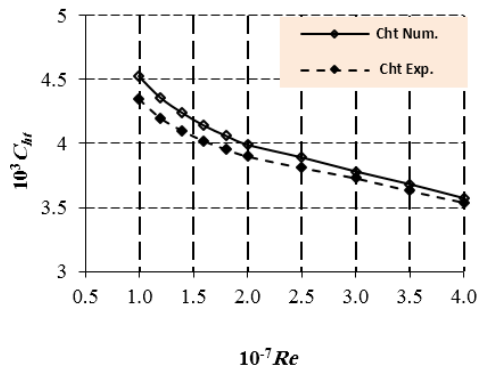


Fig. 11. Comparison experimental and calculated results for hull resistance coefficient in submergence condition

### 5.1.3 Self-Propulsion Condition

After determining performance coefficients of propeller in open water condition and hull resistance for study of hull/propeller interaction, factors of wake ( $w$ ) and thrust reduction ( $t$ ) in self-propulsion condition are computed.

One of the propeller effects behind an underwater vehicle is the increase of the hull total resistance, which is important in propeller design. This effect is represented by thrust reduction factor defined as:

$$t = 1 - \frac{R_H}{T} \quad (10)$$

In the above equation  $R_H$  is the hull drag without propeller and  $T$  is the hull drag with propeller.

Wake is the fluid velocity changes, which can have various causes. In fact, if the submarine moves with speed  $V$ , the velocity of the fluid entering the propeller is less than  $V$ .

Wake factor can be obtained from the following equation:

$$w = \frac{V - V_a}{V} \quad (11)$$

Where  $V_a$  is the actual inlet velocity to the propeller and  $V$  is the advance velocity.

In order to calculate the mentioned factors in self

propulsion condition, the total resistance at each speed is balanced by the delivered thrust of the propeller. The required propeller thrust is obtained by adjusting the rotation rate of the propeller.

The computed wake and thrust reduction factors are shown in Fig. 12. It is observed that in this range of Reynolds numbers, the maximum of the thrust reduction and wake factors are 0.157 and 0.322, respectively. According to the figure it is clear that under the considered conditions, the changes in thrust reduction and wake factors are small. This result is obvious in other researches, including N. Zhang and S. L. Zhang (2014). Considering the use of methods in numerical simulation presented in this section similar to the methods provided in previous sections, having fairly good accuracy, achieving appropriate accuracy is expected for thrust reduction and wake factor values.

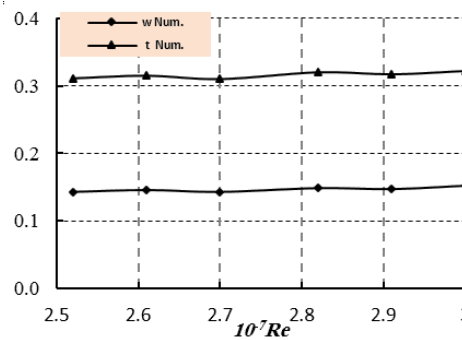


Fig. 12. Computed self-propulsion factors

The axial velocities in submergence condition at the different distances from propeller plane have been presented in Fig. 13. As seen in the figure, there are significant velocity gradients after the propeller plane. These gradients in the wake region are created by two sources namely propeller rotation and submarine hull. As can be inferred from the figure, the effect of the submarine hull on the velocity gradients is less than propeller rotation in this case. Comparing the contours of this figure shows that, by getting away from the propeller plane within the considered range ( $x = 0$  to  $x = 3R$ ), the velocity gradients increase. Also, by getting far from the propeller enough, the gradients are gradually reduced and the velocity becomes uniform.

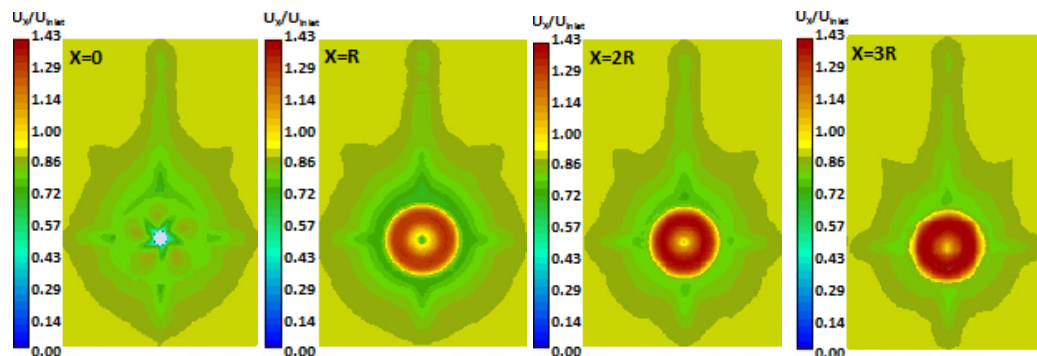


Fig. 13. Distribution of axial velocity ( $U_x/U_{inlet}$ ) at transverse planes  $X=0$ ,  $X=R$ ,  $X=2R$  and  $X=3R$  after the propeller, in submergence condition (self-propulsion point,  $Re=2.7 \times 10^7$ )

**Table 6 Uncertainty of the experimental hull resistance coefficient results in submergence Condition**

$Re \times 10^{-7}$	1.0	1.2	1.4	1.6	1.8	2.0	2.5	3.0	3.	4
$B_{Cht}$	2.94E-5	2.38E-05	2.00E-05	1.73E-05	1.54E-05	1.43E-05	1.18E-05	1.02E-05	9.02E-06	8.39E-06
$P_{Cht}$	2.28E-05	1.64E-05	1.76E-05	1.24E-05	1.53E-05	1.37E-05	5.48E-06	5.10E-06	6.00E-06	6.05E-06
$U_{Cht}$	3.72E-05	2.89E-05	2.66E-05	2.13E-05	2.17E-05	1.98E-05	1.30E-05	1.14E-05	1.08E-05	1.03E-05
$U_{Cht}/C_{ht}(\%)$	0.86	0.69	0.65	0.53	0.55	0.51	0.35	0.31	0.31	0.30

Uncertainty of the experimental results presented in this section are given in Table 6. The uncertainty of the experimental results have been obtained by calculating bias errors and standard deviations of measured values including hull geometry, carriage speed, hull resistance and temperature/ density/viscosity.

### 5.2 Surface Condition

The hull/propeller interaction of a submarine in surface condition is the topic under discussion here. For this purpose, performance coefficients of the propeller and hull resistance of the submarine are calculated, and the results have been compared with experimental ones for validation. Then, self-propulsion factors are computed.

As previously mentioned, the VOF method has been used for free surface modeling.

#### 5.2.1 Performance of Propeller near the Surface

When the submarine moves on the surface, the distance of propeller from water level is reduced. In this case, in addition to the wave making of propeller, by reducing the distance of propeller shaft to less than 1.5D, the possibility of air being drawn from the water surface is caused by the propeller performance (ITTC Recommended Procedures and Guidelines (2002c)).

The distance of the propeller shaft from water level in surface condition is considered to be 0.9D. According to subjects mentioned above, the effect of free surface is not negligible.

Therefore, calculations and experimental tests have been carried out considering the performance of the propeller near the water surface. The computed Thrust, torque and efficiency coefficients and the experimental data near the surface and in open water condition at advance ratio of 0.1-0.8 are shown in Fig. 14.

Comparing the experimental results of near surface condition with open water condition shows that reducing

the advance ratio from 0.8 to 0.1 reduces thrust and torque coefficients in near surface condition compared to open water condition, so that relative reduction of the thrust and torque coefficients are 2.3%-8.95% and 1.63%-6.5%, respectively. Also a sudden drop in thrust and torque coefficients can be seen due to the creation of ventilation phenomenon when advance ratio becomes less than 0.4. According to the computational and experimental results near the surface condition, the maximum errors of thrust and torque coefficient are 3.93% and 4.28%, respectively. This demonstrates the accuracy of the numerical method.

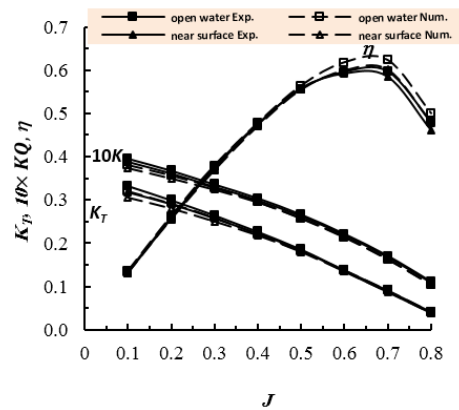


**Fig. 14. Comparison of thrust and torque coefficients in near the surface and open water condition**

The uncertainty of the experimental results presented in this section have been included in Table 7.

#### 5.2.2 Hull Resistance in near surface

In the present section, the hull resistance is investigated in the absence of the propeller. For this purpose, hull resistance of submarine at different Froude numbers (based on the hull length) are computed; then computational and experimental hull resistance coefficients are presented in Fig. 15.

**Table 7 Uncertainty of the propeller experimental results in near surface condition**

J	0.1	0.20	0.3	0.40	0.5	0.6	0.7	0.8
$B_{KT}$	2.39E-03	2.05E-03	1.75E-03	1.40E-03	1.29E-03	9.65E-04	6.67E-04	3.95E-04
$P_{KT}$	4.21E-04	3.92E-04	2.87E-04	3.11E-04	2.79E-04	1.32E-04	8.98E-05	5.86E-05
$U_{KT}$	2.42E-03	2.09E-03	1.78E-03	1.43E-03	1.32E-03	9.74E-04	6.73E-04	3.99E-04
$U_{KT}/K_T(\%)$	0.76	0.72	0.69	0.65	0.73	0.74	0.78	0.46
$B_{KQ}$	2.96E-04	2.75E-04	2.47E-04	2.14E-04	1.98E-04	1.64E-04	1.28E-04	8.87E-05
$P_{KQ}$	1.26E-04	1.05E-04	8.18E-05	9.21E-05	9.91E-05	4.32E-05	3.34E-05	2.42E-05
$U_{KQ}$	3.21E-04	2.95E-04	2.60E-04	2.33E-04	2.22E-04	1.70E-04	1.33E-04	9.19E-05
$U_{KQ}/K_Q(\%)$	0.83	0.82	0.79	0.78	0.86	0.80	0.81	0.56

The study results show that maximum computational error is about 6.3%, which represents the accuracy of numerical solution. Relative changes of experimental and computational hull resistance in surface to submergence condition ( $\Delta R$ ) at Froude numbers of 0.215 to 0.435 can be seen in Fig. 16. It shows that the amount of hull resistance force in surface condition is more than submergence condition ( $\% \Delta R$  about 29-74%). The reason is that the shape of the submarine hull for moving on the surface is not suitable and also, when the submarine moves on the surface, the wave making resistance appears and increases the hull resistance in surface condition.

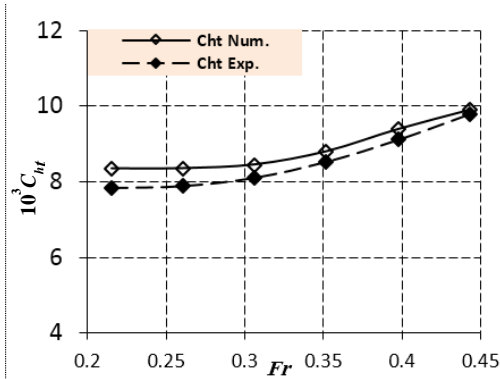


Fig. 15. Experimental and computational hull resistance coefficient in surface condition

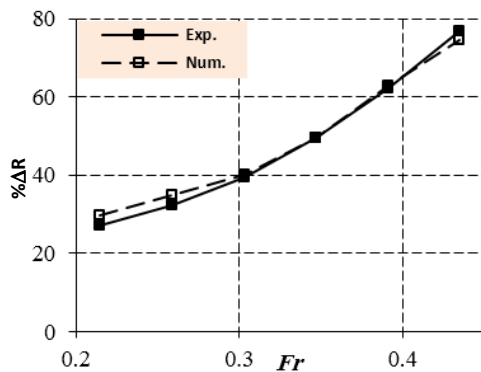


Fig. 16. Hull resistance changes in surface condition to submerged condition

The uncertainty of the experimental results obtained from the hull resistance test in surface condition have been presented in Table 8.

### 5.2.3 Self-Propulsion Condition

According to determination of hull resistance coefficients in surface condition, self-propelled factors at different Froude numbers are calculated and results are shown in Fig. 17. It is concluded that in this range of Froude numbers the maximum of thrust reduction and wake factors are 0.127 and 0.299, respectively. The values of these factors are

important in estimating the power consumption of a submarine in surface condition.

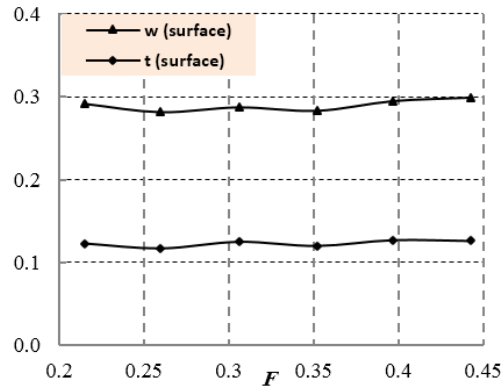


Fig. 17. Computed self-propulsion factors in surface condition

Comparison between thrust reduction and wake factors presented in Figs. 12 and 17 shows that in surface condition these factors are about 19 and 7 percent less than submergence condition, respectively.

In Fig. 18, the volume fraction variations around the submarine at the Froude numbers of 0.259, 0.347 and 0.435 are depicted. From this figure the free surfaces can be distinguished. As can be seen, the free surface in the Froude number of 0.259 is approximately flat and horizontal. However, with increasing the Froude number, some waves are produced before and after the submarine. Generally, due to the increase in the linear momentum of the flow, by increasing the axial velocity, larger waves are produced and the free surface has more distortion as the Froude number increases.

The axial velocity contours at various sections after the propeller have been shown in Fig. 19. As illustrated in this figure, it is clear that there are significant velocity gradients in the flow field. In this case, the flow field in the wake region is affected not only by propeller rotation and submarine, but also by free surface flow. Certainly, the effect of the free surface on the velocity gradients is less than the wake generated by propeller rotation and submarine hull. Investigating the contours of this figure shows that, velocity gradients and maximum axial velocity increases just the same as the results obtained in submergence condition, by getting far from propeller plane within the considered range.

The comparison of the contours presented in this figure with the contours of axial velocity in submergence condition (Fig. 13) shows that, the velocity gradients are greater in this case. Therefore more fluctuations in flow field should be expected in surface condition.

Table 8 Uncertainty of the experimental hull resistance coefficient results in surface condition

Fr	0.215	0.259	0.303	0.347	0.391	0.435
$B_{cht}$	5.45E-05	4.58E-05	4.03E-05	3.74E-05	3.62E-05	3.51E-05
$P_{cht}$	2.25E-05	2.61E-05	2.09E-05	2.02E-05	8.00E-06	1.45E-05
$U_{cht}$	5.90E-05	5.27E-05	4.54E-05	4.25E-05	3.70E-05	3.80E-05
$U_{cht}/C_{ht}(\%)$	0.71	0.63	0.54	0.48	0.39	0.38

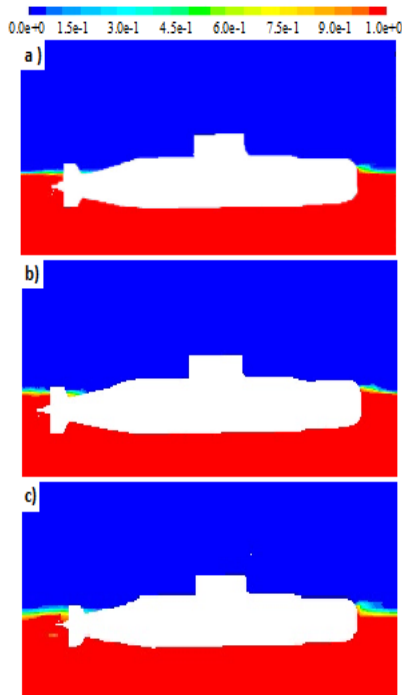


**Fig. 18. Volume fraction (water) contours around the submarine;**  
**a)  $Fr=0.259$ ; b)  $Fr=0.347$ ; c)  $Fr=0.435$**

As previously mentioned, the submarine resistance force in surface condition is more than submergence condition. As a result, submarine power consumption when moving on the surface is more than underwater. The submarine power is shown in Fig. 20 for Comparison. Comparing power consumption in surface and submergence condition shows that their values in submergence condition are less than its surface one. So that, at the same speed, power consumption in surface condition is about 45-800 (w) more than submergence condition.

## 6. CONCLUSIONS

In this paper, behaviors of a submarine and propeller models in submergence and surface conditions have been investigated using the experimental test results and also numerical methods based on RANS equations.

For validating numerical results, values of hull resistance and performance coefficients of propeller gained from numerical simulations were compared with the results of experimental tests. Comparing the results showed that computational results are in good agreement with experimental results.

According to the results of experimental tests and numerical analysis in this study it can be concluded:

- Operation of the propeller near water surface reduces the thrust coefficient of propeller compared to open water condition, such that according to the results of experiments conducted by reducing the advance ratio from 0.8 to 0.1, the relative reduction of thrust coefficients increases from 2.3% to 8.95%.
- Investigating the values of hull resistance changes in surface to submerged condition obtained in this study (about 29-74%) indicates that the amount of hull resistance force in surface condition is more than submergence condition.
- Thrust reduction factor and wake are main parameters in study of hull/propeller interaction. Comparing these two parameters in surface and submergence condition shows that their values in surface condition are less than its submergence one.

Obtained results can be useful with regard to the use of actual geometrical model of submarine in numerical simulation and also investigation of propeller performance near the surface for more accurate assessment of submarines performance in different regimes of motion.

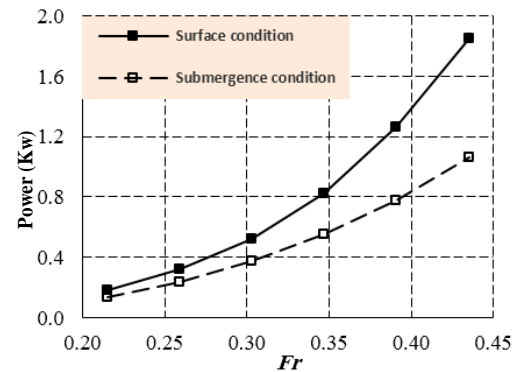


**Fig. 20. Effective power under surface and submergence condition**

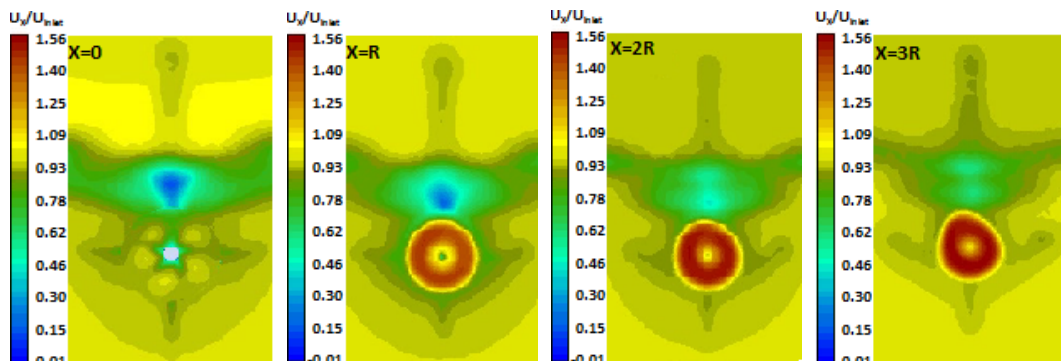


**Fig. 19. Distribution of axial velocity ( $U_x/U_{inlet}$ ) at transverse planes  $X=0$ ,  $X=R$ ,  $X=2R$  and  $X=3R$  after propeller, in surface condition (self-propulsion point,  $Fr=0.397$ )**

## REFERENCES

- Bernitsas, M. M., D. Ray, and P. Kinley (1981). *K<sub>T</sub>, K<sub>Q</sub> and efficiency curves for the wageningen b-series propellers*. Report No. 237, Department of Naval Architecture and Marine Engineering, Michigan University.
- Budak, G. and S. Beji (2016). Computational Resistance Analyses of a Generic Submarine Hull Form and Its Geometric Variants. *Journal of Ocean Technology*, 11(2), 77-86.
- Carlton, J. S. (2011). *Marine Propellers and Propulsion*. Butterworth-Heinemann.
- Chase, N. and P. M. Carrica (2013). Submarine propeller computations and application to self-propulsion of DARPA Suboff, *Ocean Engineering* 60, pp. 68–80.
- Delen, C., S. Sezen and S. Bal (2017). Computational Investigation of Self Propulsion Performance of DARPA SUBOFF Vehicle. *TAMAP Journal of Engineering*, 1-12.
- Farsi, M., Rishchri, M. S. Seif and A. H. Banisi (2007). Study on performance of the propeller in the wake field of marine vehicle with using computational fluid dynamics. In *Proceedings of Ninth Marine Industries Conference*, Noor, Iran.
- Gao, X. W. and T. G. Davies (2002). *Boundary Element Programming in Mechanics*. Cambridge University Press, New York.
- Ghassemi, H. (2003). Hydrodynamic characteristics of marine propeller in steady and unsteady wake flows. *Journal of Science and Technology of AmirKabir* 14(54), 81-98
- Gohil, P. P. and R. P. Saini (2016). Numerical Study of Cavitation in Francis Turbine of a Small Hydro Power Plant. *Journal of Applied Fluid Mechanics* 9(1), 357-365.
- Gross, A., A. Kremheller and H.F. Fasel (2011). Simulation of Flow over Suboff Bare Hull Model. *AIAA Aerospace Sciences Meeting*, Orlando, Florida.
- Hayati, A. N., S. M. Hashemi and M. Shams (2013). A study on the behind-hull Performance of marine propellers astern autonomous underwater vehicles at diverse Angles of attack. *Ocean Engineering* 59, 152-163.
- Hirt, C. W. and B. D. Nichols (1981). Volume of fluid (VOF) method for the dynamics of free boundaries. *Journal of Computational Physics* 39, 201-225.
- ITTC (2002a). *Recommended Procedures and Guidelines*. Model Manufacture, 7.5-01-01-01.
- ITTC (2002b). *Recommended Procedures and Guidelines*. Testing and Extrapolation Methods for Resistance Test, 7.5-02-02-01.
- ITTC (2002c). *Recommended Procedures and Guidelines*. Testing and Extrapolation Methods Propulsion, Performance Propulsion Test, 7.5-02-03-01.1.
- ITTC (2002d). *Recommended Procedures and Guidelines*. Testing and Extrapolation Methods Propulsion & Propulsor Open Water Test, 7.5-02-03-02.1.
- Ji, B., X. W. Luo, Y. L. Wu, S. H. Liu, H. Y. Xu and A. Oshima (2010). Numerical Investigation of Unsteady Cavitating Turbulent Flow Around a Full Scale Marine Propeller. *Journal of Hydrodynamics* 22(5), 747–752.
- Kaidi, S., H. Smaoui and P. Sergent (2017). Numerical Estimation of Bank-Propeller-Hull Interaction Effect on Ship Manoeuvring Using CFD Method. *Journal of Hydrodynamics* 29(1), 154-167.
- Kinnas, S. A. and C. Y. Hsin (1992). Boundary element method for the analysis of the unsteady flow around extreme propeller geometry. *AIAA Journal* 30(3), 688-696.
- Menter, F. R. (1994). Two-equation eddy-viscosity turbulence models for engineering applications, *AIAA Journal* 32(8), 1598-1605.
- Moonesun, M., M. Javadi, P. Charmdooz and K. U. Mikhailovich (2013). Evaluation of submarine model test in towing tank and comparison with CFD and experimental formulas for fully submerged resistance, *Indian Journal Geo-Marine Sciences* 42(8), 1049–1056.
- Nan, Z., S. Hongcui, and Y. Huizhi (2005). Numerical simulation of flow around submarine under full surface and submerged conditions. In *5th Osaka Colloquium on Advanced Research on Ship Viscous Flow and Hull Form Design by EFD and CFD Approaches*.
- Ohkusu, M. (1996). Advances in Marine Hydrodynamics, *Computational Mechanics* (5), 279-322.
- Taskar, B., K. K. Yum, S. Steen and E. Pedersen (2016). The effect of waves on engine-propeller dynamics and propulsion performance of ships. *Ocean Engineering* 122, 262-277.
- Turnock, S.R. and A. M. Wright (2000). Directly coupled fluid structural model of a ship rudder behind a propeller. *Marine Structures* 13(1), 53-72.
- Watanabe, T., T. Kawamura, Y. Takekoshi, M. Maeda and S. H. Rhee (2003). Simulation of steady and unsteady cavitation on a marine propeller using a RANS CFD code. In *Proceedings of Fifth International Symposium on Cavitation*, Osaka, Japan, 1-4.
- Zhang, N. and S. L. Zhang (2014). Numerical Simulation of Hull/Propeller Interaction of Submarine in Submergence and Near Surface Conditions. *Journal of Hydrodynamics* 26(1), 50-56.
- Zhang, Z. R. (2010). Verification and Validation for RANS Simulation of KCS Container Ship without/with Propeller. *Journal Hydrodynamics* 22(5), 932–939.